OPTICAL PROPERTIES OF ORDERED GAINP

P. ERNST*, C. GENG*, G. HAHN*, F. SCHOLZ*, H. SCHWEIZER*, YONG ZHANG**, and A. MASCARENHAS**

* 4. Physikalisches Institut, Universität Stuttgart, Pfaffendwaldring 57, 70550 Stuttgart, Germany

** National Renewable Energy Laboratory, 1617 Cole Boulevard, Golden, Colorado 80401, USA

ABSTRACT

We use the information from low temperature PLE spectra measured on a set of samples with different degree of order for an investigation of the correlation between the order dependent valence band splitting and band gap reduction. The experimental values are compared with predictions from recent *ab initio* band structure calculations.

Moreover, we show how the low temperature optical properties of ordered $GaInP_2$ are related to the microstructure of the material. We find a close correlation between the size of the ordered domains and the relative intensity of the intrinsic PL-peak from excitonic recombination compared with the rapidly shifting, below band-gap luminescence emission.

PART I: BAND-GAP REDUCTION AND VALENCE-BAND SPLITTING OF ORDERED GAINP

The phenomenon of spontaneous long-range ordering in several III-V zincblende semiconductors has been studied by a number of groups both experimentally and theoretically. In the case of $GaInP_2$, the ordered state is represented by the $CuPt_B$ structure. Growing the material by metal organic vapor phase epitaxy (MOVPE) offers a wide range of growth conditions that result in different values of the order parameter η.[1] Crystal ordering strongly affects the electronic properties of $GaInP_2$. Order-dependent band-gap reduction (BGR) and valence-band splitting (VBS) have been predicted theoretically [1] and demonstrated experimentally [2, 3].

The first quantitative theoretical predictions of VBS and BGR for perfect ordering in $GaInP_2$ were published in 1989 [1, 4]. Nevertheless, there are very few experiments published that allow us to determine simultaneously the BGR *and* VBS of a series of samples with varying order parameter. This is mainly because the results of optical spectroscopy on ordered $GaInP_2$ samples show some unusual features, which are the subject of a series of papers [5, 6, 7, 8, 9]. (1) It has been pointed out early [5] that low-temperature photoluminescence spectroscopy (PL) is not able to yield precise values for the band-gap energy because either the PL spectrum consists of several peaks that are not yet understood, or the PL peak

[1]The order parameter of $GaInP_2$ is defined by the composition of the alternating Ga-rich and In-rich monolayers: Ordered material consists of a sequence of layers $(Ga_{1+\eta}In_{1-\eta}P_2)$ and $(Ga_{1-\eta}In_{1+\eta}P_2)$ oriented perpendicularly to a [111]-direction.

Mat. Res. Soc. Symp. Proc. Vol. 417 © 1996 Materials Research Society

Downloaded from https://www.cambridge.org/core. Univ. of North Carolina at Charlotte, on 03 Aug 2018 at 16:19:56, subject to the Cambridge Core terms of use, available at https://www.cambridge.org/core/terms. https://doi.org/10.1557/PROC-417-19

moves with varying excitation density and shows an extremely large Stokes shift. (2) On the other hand, even photoluminescence excitation spectroscopy (PLE) was unable to yield a precise measure of the band-gap of ordered samples, because no sharp excitonic maxima were detected. This latter phenomenon was attributed to an inhomogeneity in order parameter η within the samples [10].

We present a study of the correlation between BGR and VBS based on low-temperature PLE spectra. The high quality of our samples results in clearly resolved excitonic maxima of both valence band edges and allows for a direct determination of the splitting in the valence band and the excitonic transition energy of a series of samples. These data are compared with recent band structure calculations by Wei, Mäder, and Zunger [1, 11, 12, 13, 14, 15].

We have grown a series of samples of bulk $GaInP_2$ by means of low-pressure MOVPE, as described in more detail in [9]. The degree of ordering is influenced by varying the growth temperature between 660 °C and 840 °C, the substrate misorientation (6° $\rightarrow [111]_A$ and 6°, 10°, 15° $\rightarrow [111]_B$), and the growth rate ($0.5 \ldots 2.0\,\mu$m/h). The V/III ratio was kept constant at 240. As can be seen in table 1, the order parameters cover the range from $\eta = 0.0$ to $\eta \approx 0.55$.

Sample No.	Substrate	T_g [°C]	E_x [eV]	ΔE_{VBS} [meV]	η
1	6° $\rightarrow [111]_A$	840	2.007	0	0.0
2	6° $\rightarrow [111]_A$	810	2.009	0	0.0
3	6° $\rightarrow [111]_A$	750	1.988	3.5	0.23
4	6° $\rightarrow [111]_A$	720	1.976	6.9	0.23
5	15° $\rightarrow [111]_B$	690	1.973	7.6	0.24
6	6° $\rightarrow [111]_A$	690	1.973	10.0	0.28
7	6° $\rightarrow [111]_A$	660	1.973	11.0	0.30
8	6° $\rightarrow [111]_A$	660	1.971	11.8	0.31
9	6° $\rightarrow [111]_B$	750	1.957	11.3	0.32
10	10° $\rightarrow [111]_B$	690	1.916	21.0	0.43
11	6° $\rightarrow [111]_B$	720	1.914	21.7	0.44
12	6° $\rightarrow [111]_B$	690	1.893	26.5	0.49
13	6° $\rightarrow [111]_B$	660	1.886	26.8	0.50
14	6° $\rightarrow [111]_B$	690	1.885	27.7	0.51
15	6° $\rightarrow [111]_B$	660	1.879	29.5	0.54

Table 1: Samples of bulk $GaInP_2$ used in this work. Substrate misorientation and growth temperature T_g have been varied to obtain different order parameters η. The measured (and corrected) values of E_x and ΔE_{VBS} are given in column 5 and 6. η is calculated from ΔE_{VBS} using equations 1 and 2.

Fig. 1 shows typical PLE spectra from an ordered sample. Two absorption maxima are clearly resolved. As described in the figure caption they show the expected dependence on the polarization of the incident light. The spectra, which are all taken at $T = 2\,$K, allow us to determine the parameters E_x and ΔE_{VBS} with an uncertainty of less than 1 meV, E_x being the $k = 0$ transition energy of the free (heavy-hole-like) exciton (correlated with the upper valence band, $\Gamma^V_{4,5}$), and ΔE_{VBS} being the energy separation between that latter exciton and the one that is formed with the lower valence band $\Gamma^V_6(2)$ (light-hole-like).

The measured values of E_x and ΔE_{VBS} can be influenced by compositional fluctuations from

Downloaded from https://www.cambridge.org/core. Univ. of North Carolina at Charlotte, on 03 Aug 2018 at 16:19:56, subject to the Cambridge Core terms of use, available at https://www.cambridge.org/core/terms. https://doi.org/10.1557/PROC-417-19

sample to sample due to (1) the band-gap dependence on composition, and (2) the influence of strain on the band-edges. This uncertainty has been eliminated by measuring the lattice mismatch between each of the films and the GaAs-substrate by means of high-resolution X-ray diffractometry (room temperature). In each case, the lattice mismatch was found to be below 10^{-3}. Using a theoretical correlation between lattice mismatch and band-gap as calculated by Krijn [16], we have determined the correction on E_x for a fictitious composition of $x_{\mathrm{Ga}} = 0.520$. This is the composition used by most other authors. The strain effect on ΔE_{VBS} due to a deviation from the strain-free composition has also been corrected. This has been done by applying a perturbative calculation method as used in [13].

Table 1 and Fig. 2 contain values of E_x and ΔE_{VBS} *after* correction.

Moreover, the measured parameters E_x and E_{VBS} are possibly influenced by a variation of the excitonic binding energy E_B^{ex} with η, and a difference in E_B^{ex} for the two excitons formed with the upper and the lower valence bands. We have recently calculated the conduction band and valence band effective masses m^* in $GaInP_2$ as a function of the order parameter using an eight-band $k{\cdot}p$ model [17]. The effective masses are found to be anisotropic between the directions parallel and perpendicular to the ordering axes (i.e. $[1\bar{1}1]$ or $[11\bar{1}]$). Using the m^* obtained in [17], we applied a variational method [18] to calculate exciton binding energies for the heavy-hole-like (hh) and the light-hole-like (lh) bands. We find that (1) E_B^{ex} for both exciton states only varies by about 1 meV with η. The calculated values are: $E_B^{ex}(\eta = 0) = 6.2\,\mathrm{meV}$, $E_B^{ex}(\eta = 1) = 5.3\,\mathrm{meV}$. (2) The difference in E_B^{ex} between the two excitons is very small ($\sim 0.1\,\mathrm{meV}$), because m^* along the ordering direction is heavier for the hh states and, on the other hand, in the plane perpendicular to the ordering direction, is heavier for the lh states, and the mass anisotropy is relatively small for the conduction

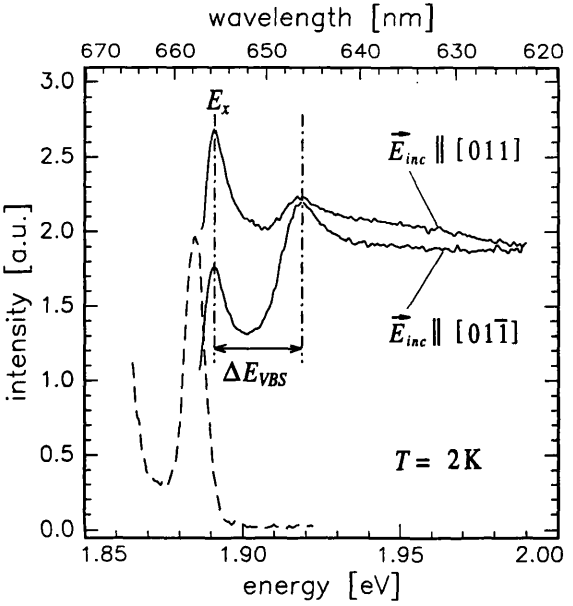

Figure 1: Typical PLE spectra from an ordered sample (sample #12). The corresponding PL is plotted with dashed lines. The two PLE spectra are taken with different polarization of the exciting laser light with respect to the ordering planes. As predicted by theory, the optical transition with the upper valence band is stronger for optical polarization parallel to the ordering planes ($\vec{E}_{inc} \parallel [011]$).

Downloaded from https://www.cambridge.org/core. Univ. of North Carolina at Charlotte, on 03 Aug 2018 at 16:19:56, subject to the Cambridge Core terms of use, available at https://www.cambridge.org/core/terms. https://doi.org/10.1557/PROC-417-19

band (which has lighter mass than the valence bands).

Both results (1) and (2) show that the measured paramters E_x and ΔE_{VBS} can be used as a valuable measure for the band-gap energy E_G and the valence-band splitting, respectively, without being corrected for exciton binding energy effects. We therefore set $E_x = E_g$ in the following.

Fig. 2 shows a plot of the (composition corrected) values of E_g and ΔE_{VBS} of the samples listed in table 1. The dotted and dashed lines represent theoretical predictions by Wei, Mäder, and Zunger [12, 13, 14, 15]. They are calculated using the following equations:

$$\begin{aligned} E_g(\eta) &= E_g^{(\eta=0)} - \Delta E_g^{(\eta=1)} \cdot \eta^2 \\ \Delta E_{VBS}(\eta) &= E_1(\eta) - E_2(\eta) \; . \end{aligned} \tag{1}$$

The valence-band maxima E_1 and E_2 can be calculated as a function of η by means of the formulas given in [12]:

$$\begin{aligned} E_1 &= \frac{1}{2}(\Delta_0 + \Delta_{CF}) \\ E_2 &= \frac{1}{2}\left((\Delta_0 + \Delta_{CF})^2 - \frac{8}{3}\Delta_0\Delta_{CF}\right)^{1/2} \; , \end{aligned} \tag{2}$$

with the spin-orbit splitting and crystal-field splitting parameters Δ_0 and Δ_{CF}. These parameters also depend quadratically on η; values for $\eta = 0$ and $\eta = 1$ for both parameters are given in [12]. Elimination of η in equations 1 leads to the correlation between E_g and ΔE_{VBS} that is used in Fig. 2.

As discussed in [12], the crystal-field splitting parameter $\Delta_{CF}^{(\eta=1)}$ depends on whether the rhombohedral distortion along [111] of the ordered CuPt structure is relaxed (rhombohedral

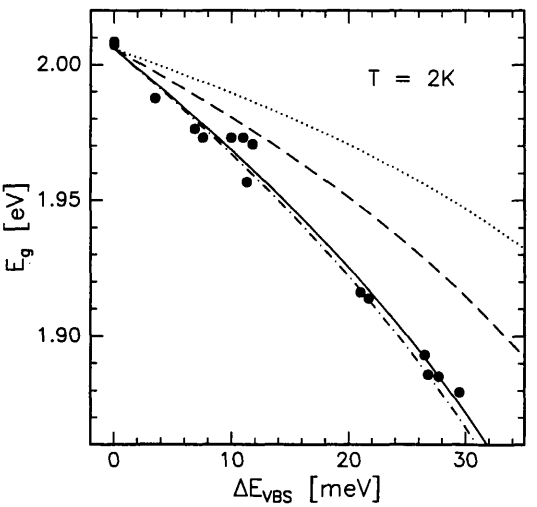

Figure 2: *Solid points:* Values of E_g and ΔE_{VBS} of our samples. *Dotted and dashed lines:* Prediction by Wei and Zunger [12, 13], calculated with the parameters $E_g^{(0)} = 2.005\,\text{eV}$, $\Delta E_g^{(1)} = 320\,\text{meV}$, and $\Delta_{CF}^{(1)} = 200\,\text{meV}$ (dashed), and $\Delta_{CF}^{(1)} = 310\,\text{meV}$ (dotted). *Dash-dotted line:* Prediction by Mäder and Zunger [14, 15]. Parameters: $E_g^{(0)} = 2.005\,\text{eV}$, $\Delta E_g^{(1)} = 490\,\text{meV}$, and $\Delta_{CF}^{(1)} = 200\,\text{meV}$. *Solid line:* Best Fit to the data.

Downloaded from https://www.cambridge.org/core. Univ. of North Carolina at Charlotte, on 03 Aug 2018 at 16:19:56, subject to the Cambridge Core terms of use, available at https://www.cambridge.org/core/terms. https://doi.org/10.1557/PROC-417-19

structure, $\Delta_{CF}^{(1)} = 310\,\text{meV}$) or unrelaxed (cubic structure, coherent with the (100) GaAs-substrate, $\Delta_{CF}^{(1)} = 200\,\text{meV}$). It can be seen in Fig. 2 that the dotted line, which is plotted for a relaxed structure, lies clearly above the data points. This suggests that the ordered material is realized as a cubic layer (unrelaxed), i.e. the epitaxial film is grown in coherence with the substrate. This is in good agreement with results from diffractometry. The other theoretical curves, as well as our fit, therefore assume $\Delta_{CF}^{(1)} = 200\,\text{meV}$.

The calculations by Wei and Zunger lead to a maximum band-gap reduction of $\Delta E_G^{(1)} = 320\,\text{meV}$. More recent calculations by Mäder and Zunger, however, gave $\Delta E_G^{(1)} = 490\,\text{meV}$. Curves corresponding to both values (represented by the dashed (Wei) and the dash-dotted (Mäder) lines) are compared with our data in Fig. 2. Because both theoretical values do not yield exact agreement with the experimental data, we have used the correlation $E_G = f(\Delta E_{VBS})$, as given by equations 1 and 2, to fit the paramter $\Delta E_G^{(1)}$. The best fit was achieved with $\Delta E_G^{(1)} = 471\,\text{meV} \pm 12\,\text{meV}$, represented by the solid line in Fig. 2. Thus the ratio $\Delta E_G^{(1)}/\Delta_{CF}^{(1)}$, which is independent of the exact value of $\Delta_{CF}^{(1)}$, is found to be 2.36 ± 0.06. This result suggests that the more recent theoretical value of $\Delta E_G^{(1)} = 490\,\text{meV}$ is more close to experiment than the earlier value. Moreover, we point out that the value calculated by Kurimoto and Hamada [4] is definitely too low. These authors predicted a total band-gap reduction of 150 meV for perfectly ordered $GaInP_2$.

Previously, the theoretical prediction of BGR and VBS of ordered $GaInP_2$ has been compared [13] with experimental results by Alonso et al. [19]. If we fit the function $E_G = f(\Delta E_{VBS})$ used above to these data, we get a value of $\Delta E_G^{(1)} = 406\,\text{meV} \pm 28\,\text{meV}$. It can be seen from the higher variance that these data are much more influenced by scattering than ours. Especially, the data points from stronger ordered samples scatter considerably, which makes the extrapolation to perfect ordering ($\eta = 1$) very difficult. Moreover, Alonso et al. had to use a fitting procedure to evaluate the band-gap values from their reflectance spectra, a procedure that may introduce systematic errors. Note that our data are based directly on the measured PLE spectra, without any numerical treatment of the data (except from composition correction).

PART II: CORRELATION BETWEEN THE MICROSTRUCTURE OF ORDERED GAINP AND ITS PHOTOLUMINESCENCE PROPERTIES

In this chapter, we want to focus on some properties of ordered $GaInP_2$ which are not yet fully understood in terms of the microstructure of the ordered alloy. In particular, low-temperature photoluminescence (PL) spectra of this material are dominated by a peak that comes from below-band-gap transitions (10...50 meV below the fundamental band gap) and moves to higher emission energy with increasing excitation intensity ("moving" emission). Previous work [5, 6, 7, 8, 20, 9] has established the following facts about this PL feature. (1) It is not due to usual donor or acceptor states (impurities) with well-defined binding energies, because (a) its dependence on excitation intensity is much stronger than expected for a donor- or acceptor-related optical transition [21, 22], and (b) it vanishes with decreasing order parameter [9], although an impurity would also appear in the disordered material. (2) There is no absorption of light in the energy range of the moving emission. Instead, PLE spectra monitored with detection energies positioned at the moving emission

Downloaded from https://www.cambridge.org/core. Univ. of North Carolina at Charlotte, on 03 Aug 2018 at 16:19:56, subject to the Cambridge Core terms of use, available at https://www.cambridge.org/core/terms. https://doi.org/10.1557/PROC-417-19

show the same band-edge as those monitored on the free exciton [9]. (3) The lifetime of the moving emission is extremely long and depends strongly on the detection energy [6, 7, 9]. (4) With increasing temperature, the moving emission first shifts to higher energy, then loses intensity compared with the direct band-gap PL, and finally disappears completely [5, 20]. At room temperature, only direct band-band recombination is observed, as expected from any semiconductor with a direct band-gap.

On the other hand, transmission electron miscroscopy (TEM) studies have shown that the microstructure of ordered $GaInP_2$ often consists of domains of ordered material, embedded in a more disordered matrix [23, 24]. The size of the ordered domains seen in dark-field images stongly depends on growth conditions and may range from 10 nm up to 1μm (lateral width) [25, 26].

The aim of this investigation is to show (1) how the domain size depends on the growth temperature, which is the only growth parameter varied here, and (2) that there is a close correlation between the average domain size in an ordered sample and its optical properties as measured by low-temperature PL and excitation spectroscopy (PLE).

Experimental

We have grown a series of four samples of bulk $GaInP_2$ by means of low-pressure MOVPE, described in more detail in [9]. The degree of ordering was controlled by varying the growth temperature between 630 °C and 750 °C. Each sample was grown on a (100) GaAs-substrate misoriented 6° off towards $[111]_B$. The growth rate was 2.0 μm/h at a V/III ratio of 240. The layer thickness of each sample is 2 μm.

The TEM-investigations have been performed using [011] cross-section slides. The slides have been prepared by gluing two GaInP surfaces together (in a stack of Si wafer pieces for better stability). Discs with a thickness of 500 μm were cut perpendicularly to the layers and mechanically polished to a thickness of 100 μm. Then, hemispherical dimpels were created on the glue line by means of a rotating copper wheel (dimpler). A second chemical polishing was carried out in a solution of H_2SO_4 : H_2O_2 : H_2O (3:1:1) for 60 s at a temperature of 43 °C. Finally, the slides were thinned in an Ar^+-beam at the temperature of liquid nitrogen.

The images have been taken with the electron-beam oriented along the crystal's [011]-direction, with a spot size on the sample of about 1 μm for diffraction patterns and 5 μm for dark-field images. The dark-field images have been taken using the $\frac{1}{2}(3\bar{1}1)$-reflex, because the $\frac{1}{2}(1\bar{1}1)$-reflex yielded images with a poor contrast caused by some background intensity of the direct beam.

Optical measurements were performed using an argon ion laser operated in multiline mode (with main laser lines at 488 nm and 514 nm) for PL and a tunable dye laser filled with DCM (available wavelength range: 610 ... 700 nm) for PLE. Luminescence was dispersed by an 0.85 m double monochromator and detected by a cooled InGaAs photomultiplier.

Downloaded from https://www.cambridge.org/core. Univ. of North Carolina at Charlotte, on 03 Aug 2018 at 16:19:56, subject to the Cambridge Core terms of use, available at https://www.cambridge.org/core/terms. https://doi.org/10.1557/PROC-417-19

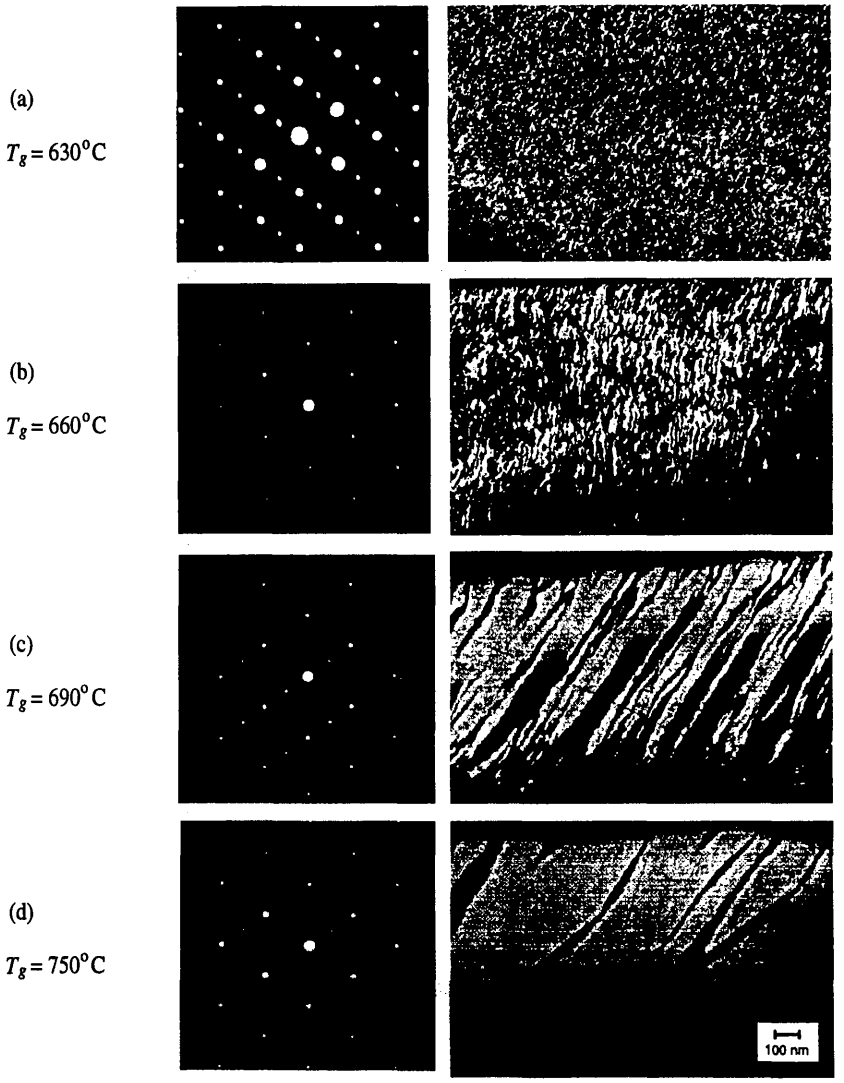

Figure 3: TED patterns (left) and DF-TEM images (right) of the samples grown at 630 °C, 660 °C, 690 °C, and 750 °C. The superlattice spot that has been used to create the dark-field images is marked by a white circle in Fig. (c), left. The superspot labels in this image, however, differ from those used in the text. In the figure, we use the denominations common in electron microscopy that assume a [110] cross-section slide of a sample with a (001) growth direction.

Downloaded from https://www.cambridge.org/core. Univ. of North Carolina at Charlotte, on 03 Aug 2018 at 16:19:56, subject to the Cambridge Core terms of use, available at https://www.cambridge.org/core/terms. https://doi.org/10.1557/PROC-417-19

Results

Fig. 3 shows the diffraction pattern (left) and the dark-field images (right) obtained from the four samples grown at 630 °C, 660 °C, 690 °C, and 750 °C. Each of the diffraction pattern shows clear superlattice spots of only *one* ordering variant, as to be expected from the chosen substrate misorientation. The main feature of the series of DF-TEM pictures on the right of Fig. 3 is the important change in domain size with varying growth temperature. The order domains are extended in a direction almost parallel to a (111)-plane in the case of samples (c) and (d), and are nearly parallel to the growth-direction in samples (a) and (b). The lateral domain size varies systematically from about 10 nm in sample (a) to $\sim$ 500 nm in sample (d) (Fig. 4).

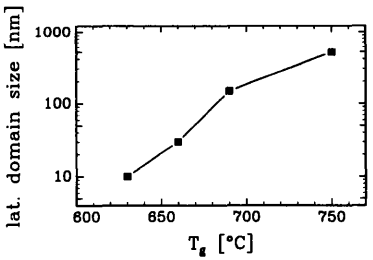

Figure 4: Typical lateral domain size of the samples as a function of the growth temperature T_g.

Now we turn to the optical data obtained from these samples. Fig. 5 shows both PL (dashed) and PLE spectra (solid), taken at $T = 2$ K. All spectra are plotted on the same energy scale to enable a direct comparison of peak energies and linewidths. The PL spectra are taken with an excitation intensity of 5 W/cm^2.

The samples grown at 750 °C and 690 °C (samples (c) and (d)) show two PL peaks. The low-energy (LE) PL peak of both samples moves to higher emission energies with increasing excitation intensity (by 5.0 meV/decade (c) and by 1.3 meV/decade (d)), whereas the high-energy (HE) peak is stationary. The linewidths of the HE peaks are 6.8 meV and 5.0 meV for samples (c) and (d), respectively, and the linewidths of the LE peaks are 10.7 meV (c) and 8.5 meV (d). In sample (d) the HE peak is dominant, whereas this peak is quite weak in sample (c). The PLE spectra A and B are monitored at the positions indicated by arrows, respectively. Excitonic absorption resonances correlated with both valence-band edges are clearly resolved in samples (d) and (c); their energetic positions are indicated by dash-dotted lines. Comparison of PL and PLE spectra points to the fact that the HE peak represents the intrinsic (excitonic) band-band recombination (the Stokes-Shifts for samples (c) and (d) are 8.8 meV and 4.5 meV, respectively). The origin of the (moving) LE peaks, on the other hand, is still unclear.

We now turn to samples (a) and (b), grown at lower temperatures. Here the (excitonic) HE emission vanishes and the single 15 – 17 meV broad PL line shows all the features of the above-mentioned LE peak: It moves with increasing exciation intensity, it shows long, detection energy dependent liftetimes, and it shows the inverted-S behavior [9]. PLE spectra, detected at the peak maximum and at the low energy flank, show smoothly rising flanks without sharp excitonic maxima. Nevertheless, the separation of the two valence-band edges can be estimated (cf. the dash-dotted lines).

Downloaded from https://www.cambridge.org/core. Univ. of North Carolina at Charlotte, on 03 Aug 2018 at 16:19:56, subject to the Cambridge Core terms of use, available at https://www.cambridge.org/core/terms. https://doi.org/10.1557/PROC-417-19

So far, we conclude that the PL intensity of the intrinsic HE luminescence peak compared with the LE peak decreases with decreasing domain size (cf. Fig. 3 and Fig. 4), and even vanishes completely at a critical domain size (lying between 30 nm and 150 nm).

However, it could be argued that the extinction of the intrinsic recombination in some samples could be due to a poor overall sample quality, e.g. high impurity concentrations, rather than the domain size. Therefore, we have made the following experiment on sample (c): It can be seen from Fig. 3 (c, right) that the size of the ordered domains varies throughout the layer. It is largest near the sample surface (top), and becomes smaller closer to the substrate (bottom). We have etched part of the epilayer to different depths on four different pieces of this sample and repeated the PL measurements on the leftover material. Etching was done by a low-damage ECR-RIE dry-etching process using an Ar/CCl_2F_2 gas mixture, as described in detail in [27]. The etching rate was 34 nm/min.

Fig. 6 shows the result. The amplitude of the LE peak is normalized to unity in each of the spectra, and each spectrum is plotted on the same y-axis. Thus, the relative quantum efficiency of the direct (excitonic) recombination can be directly seen in the intensity of the HE-peak. The peak ratio, as determined from spectra (a) to (e) of Fig. 6 by integrating the areas under the peaks, is plotted against the remaining layer thickness d in Fig. 7. We attribute the decrease of the relative quantum efficiency of the direct recombination with decreasing layer thickness to a decrease of the average domain size in the epilayer under investigation, in analogy with the above-described results from different samples with different domain sizes.

Discussion

We conclude from these experiments that the indirect transition in ordered GaInP is correlated with the domain size as determined by TEM dark-field images. In this section, we

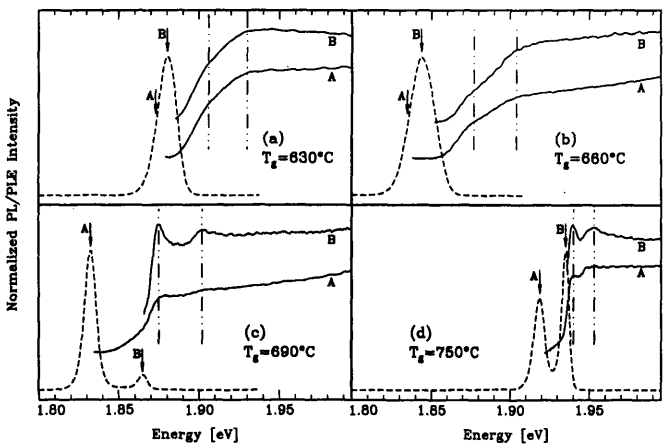

Figure 5: PL (dashed) and PLE (solid), taken at $T = 2$ K. Arrows indicate the detection energies of the corresponding PLE-spectra. The order-induced valence-band splitting can be seen in the PLE spectra either by two clearly resolved excitonic peaks ((c) and (d)), or as weak shoulders in the slopes ((a) and (b)), as indicated by dash-dotted lines. The PLE spectra are shifted on the y-axis.

Downloaded from https://www.cambridge.org/core. Univ. of North Carolina at Charlotte, on 03 Aug 2018 at 16:19:56, subject to the Cambridge Core terms of use, available at https://www.cambridge.org/core/terms. https://doi.org/10.1557/PROC-417-19

discuss different possible explanations for the indirect transitions based on the experimental evidence gathered so far.

(1) Some experiments on orderd GaInP have been interpreted by assuming a variation in order parameter through the sample volume [10, 28] together with a type-II band-offset between regions of different degrees of order [29, 30, 6, 7, 31, 32]. This situation leads to a localization of photoexcited electrons in domains of higher order parameter, whereas holes tend to relax into regions of lower order parameter. Indirect recombination processes between these spacially separated regions give rise to luminescence with photon energies below the fundamental band-gap. This scenario is consistent with all the reported features of the low energy emission, such as long lifetimes, absence of absorption, and shift to higher energy with increasing carrier density (due to a saturation of the transitions) [9].

Our experiments on the domain size also support this interpretation. If we assume that the domains that can be seen in the dark-field images differ slightly in their degree of order, then we expect indirect transitions to occur at domain boundaries. As the density of domain boundaries in the volume increases with decreasing domain size, we expect the indirect transition to become more important. This is actually observed. For very small domains (exciton diffusion radius or smaller), we do not even have a well-defined band-gap any more, which explains th absence of the HE peak and the smeared-out PLE spectrum of our samples grown at 660 °C and 630 °C. However, we cannot directly prove that the LE peak comes from domain boundaries using the experiments described above. This is currently being investigated. It is also possible that there are order parameter variations on a length scale different from the one seen in the domain images. Then, however, this length scale is different in the four samples investigated here, in similarity with the domain sizes.

(2) In two recent theoretical papers, Mäder and Zunger report on the effects of clustering on the optical properties of III-V alloys [14, 15]. Besides a band-gap reduction, the authors predict (in the case of $GaInP_2$) a type-II-like band-alignment between Ga-rich and In-rich clusters. According to these calculations, the electron wave-functions should be localized on Ga-rich sites, whereas holes are localized on In-rich regions. These clusters are therefore able to act as isolectronic traps for both electrons and holes. These traps are likely to occur with varying "binding energy." They provide another possible explanation for trapping and separation of electrons and holes and subsequent spatially indirect transition.

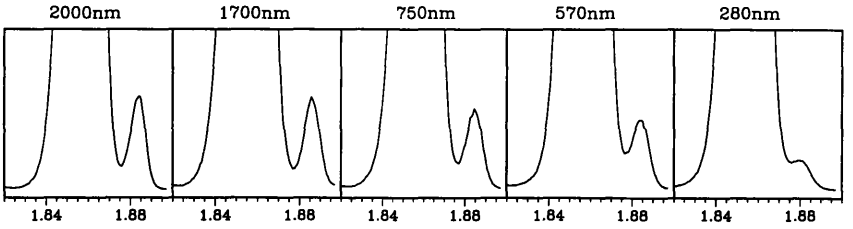

Figure 6: PL spectra of the sample grown at 690 °C, after etching down a part of the epilayer. The PL of the as-grown sample is shown in Fig. (a). The remaining thickness d of the layers after etching is given in each figure.

Downloaded from https://www.cambridge.org/core. Univ. of North Carolina at Charlotte, on 03 Aug 2018 at 16:19:56, subject to the Cambridge Core terms of use, available at https://www.cambridge.org/core/terms. https://doi.org/10.1557/PROC-417-19

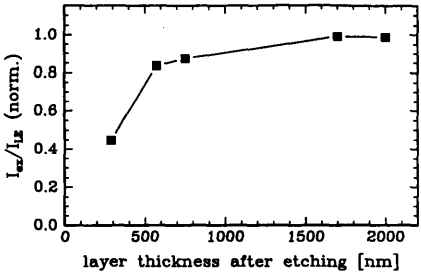

Figure 7: Relative quantum efficiency of the direct band-band recombination at low temperature as a function of the remaining layer thickness d.

If clustering is the explanation of the moving low-energy emission, we have to conclude from our experiments that (a) clusters are located at domain boundaries, or (b) their volume density in different samples is correlated with the domain size. This would have to be explained by the thermodynamics of the growth process which control both the size of ordered domains and the occurance of compositional fluctuctuations, i.e. clusters.

[1] S.-H. Wei and A. Zunger. *Phys. Rev. B* **39**, 3279 (1989).

[2] A. Gomyo, T. Suzuki and S. Iijima. *Phys. Rev. Lett.* **60**, 2645 (1988).

[3] A. Mascarenhas, S. Kurtz, A. Kibbler and J. M. Olson. *Phys. Rev. Lett.* **63**, 2108 (1989).

[4] T. Kurimoto and N. Hamada. *Phys. Rev. B* **40**, 3889 (1989).

[5] M. Kondow and S. Minagawa. *Appl. Phys. Lett.* **54**, 1760 (1989).

[6] J. E. Fouquet, V. M. Robbins, J. Rosner and O. Blum. *Appl. Phys. Lett.* **57**, 1566 (1990).

[7] M. C. DeLong, W. D. Ohlsen, I. Viohl, P. C. Taylor and J. M. Olson. *J. Appl. Phys.* **70**, 2780 (1991).

[8] M. C. DeLong, D. J. Mowbray, R. A. Hogg, M. S. Skolnick, M. Hopkinson, J. P. R. David, P. C. Taylor, S. R. Kurtz and J. M. Olson. *J. Appl. Phys.* **73**, 5163 (1993).

[9] P. Ernst, C. Geng, F. Scholz and H. Schweizer. *Phys. stat. sol. (b)* **193** (1996). In print.

[10] G. S. Horner, A. Mascarenhas, R. G. Alonso, S. Froyen, K. A. Bertness and J. M. Olson. *Phys. Rev. B* **49**, 1727 (1994).

[11] S.-H. Wei and A. Zunger. *Appl. Phys. Lett.* **56**, 662 (1990).

[12] S.-H. Wei, D. B. Laks and A. Zunger. *Appl. Phys. Lett.* **62**, 1937 (1993).

Downloaded from https://www.cambridge.org/core. Univ. of North Carolina at Charlotte, on 03 Aug 2018 at 16:19:56, subject to the Cambridge Core terms of use, available at https://www.cambridge.org/core/terms. https://doi.org/10.1557/PROC-417-19

[13] S.-H. Wei and A. Zunger. *Phys. Rev. B* **49**, 14337 (1994).

[14] K. A. Mäder and A. Zunger. *Appl. Phys. Lett.* **64**, 2882 (1994).

[15] K. A. Mäder and A. Zunger. *Phys. Rev. B* **51**, 10462 (1995).

[16] M. P. C. M. Krijn. *Semicond. Sci. Technol.* **6**, 27 (1991).

[17] Yong Zhang and A. Mascarenhas. *Phys. Rev. B* **51**, 13162 (1995).

[18] C. Kittel and A. H. Mitchell. *Phys. Rev.* **96**, 1488 (1954).

[19] R. G. Alonso, A. Mascarenhas, G. S. Horner, K. A. Bertness, S. R. Kurtz and J. M. Olson. *Phys. Rev. B* **48**, 11833 (1993).

[20] F. A. J. M. Driessen, G. J. Bauhuis, S. M. Olsthoorn and L. J. Giling. *Phys. Rev. B* **48**, 7889 (1993).

[21] J. Chevallier and A. Laugier. *Phys. stat. sol. (a)* **8**, 437 (1971).

[22] E. Zacks and A. Halperin. *Phys. Rev. B* **6**, 3072 (1972).

[23] M. Kondow, H. Kakibayashi and S. Minegawa. *J. Crystal Growth* **88**, 291 (1988).

[24] P. Bellon, J. P. Chevalier, E. Augarde, J. P. André and G. P. Martin. *J. Appl. Phys.* **66**, 2388 (1989).

[25] L. C. Su, I. H. Ho and G. B. Stringfellow. *J. Appl. Phys.* **75**, 5135 (1994).

[26] L. C. Su, I. H. Ho and G. B. Stringfellow. *J. Appl. Phys.* **76**, 3520 (1994).

[27] J. Hommel, F. Schneider, M. Moser, C. Geng, F. Scholz and H. Schweizer. *Microelectron. Eng.* **23**, 349 (1994).

[28] K. Sinha, A. Mascarenhas, G. S. Horner, K. A. Bertness, S. R. Kurtz and J. M. Olson. *Phys. Rev. B* **50**, 7509 (1994).

[29] R. P. Schneider, Jr., E. D. Jones and D. M. Follstaedt. *Appl. Phys. Lett.* **65**, 587 (1994).

[30] E. D. Jones, D. M. Follstaedt, H. Lee, J. S. Nelson and R. P. Schneider, Jr. In *22nd International Conference on the Physics of Semiconductors*, edited by D. J. Lockwood. World Scientific, Singapore 1995.

[31] J. E. Fouquet, M. S. Minsky and S. J. Rosner. *Appl. Phys. Lett.* **63**, 3212 (1993).

[32] C. Geng, P. Ernst, D. Haase, G. Hahn, F. Phillipp, A. Dörnen, H. Schweizer and F. Scholz. *6th European Workshop on MOVPE, Gent, Belgium* (1995).

Downloaded from https://www.cambridge.org/core. Univ. of North Carolina at Charlotte, on 03 Aug 2018 at 16:19:56, subject to the Cambridge Core terms of use, available at https://www.cambridge.org/core/terms. https://doi.org/10.1557/PROC-417-19